Available online at www.sciencedirect.com
SCIENCE DIRECT®
Bioorganic & Medicinal Chemistry Letters 16 (2006) 4339–4344
Bioorganic & Medicinal Chemistry Letters

Structure–activity relationships of triazolopyridine oxazole p38 inhibitors: Identification of candidates for clinical development

Kim F. McClure,* Michael A. Letavic,† Amit S. Kalgutkar, Christopher A. Gabel,‡ Laurent Audoly,§ John T. Barberia, John F. Braganza, Demetrius Carter, Thomas J. Carty, Santo R. Cortina, Mark A. Dombroski, Kathleen M. Donahue, Nancy C. Elliott, Colleen P. Gibbons, Crystal K. Jordan, Alexander V. Kuperman, Jeff M. Labasi, Ronald E. LaLiberte, Jennifer M. McCoy, Brian M. Naiman, Kendra L. Nelson, Hang T. Nguyen, Kevin M. Peese, Francis J. Sweeney, Timothy J. Taylor, Catherine E. Trebino, Yuriy A. Abramov, Ellen R. Laird, Walter A. Volberg, Jun Zhou, Justin Bach and Franco Lombardo

Pfizer Global Research and Development, Groton Laboratories, Eastern Point Road, Groton, CT 06340, USA

Received 12 April 2006; revised 15 May 2006; accepted 16 May 2006
Available online 12 June 2006

Abstract—The synthesis, structure–activity relationship, in vivo activity, and metabolic profile for a series of triazolopyridine-oxazole based p38 inhibitors are described. The deficiencies of the lead structure in the series, CP-808844, were overcome by changes to the C4 aryl group and the triazole side-chain culminating in the identification of several potential clinical candidates.

Since the discovery of p38 kinase in the mid-1990s[1] the promise of p38 inhibitors as potential therapy for diseases mediated by the overproduction of pro-inflammatory cytokines has yet to be realized. This is certainly not due to a lack of effort.[2] A clear potential source of failure lies with poorly predicting the translation of pharmacology from in vitro assays and animal models to human. For p38 this is complicated by the fact that no direct measures of p38 inhibition are yet possible in vivo.[3] Although methods are under development[4] that are mechanistically close[5] to the action of p38, the most common techniques involve measurement of downstream markers such as TNF-α from blood after exogenous stimulation.

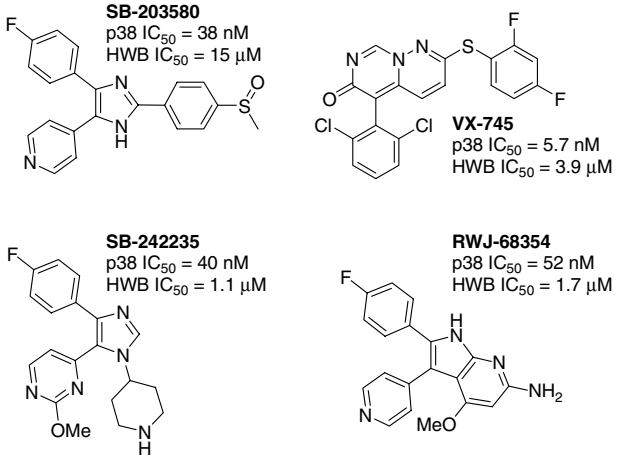

Figure 1. Enzyme and human whole blood IC_{50}s for literature compounds.[12]

Keywords: p38 kinase; MAP, mitogen activated protein; Inhibitor; SAR, structure–activity relationship; Clinical candidate; Triazolopyridine; Oxazole; Triazole; TNF-α, tumor necrosis factor-α; CP-808844; Inflammation; Arthritis; Cytokine; Anti-inflammatory.
* Corresponding author. Tel.: +1 860 441 8223; fax: +1 860 715 4610; e-mail: kim.f.mcclure@pfizer.com
† Present address: Johnson & Johnson PRD-La Jolla, 3210 Merryfield Row, San Diego, CA 92121-1126, USA.
‡ Present address: Amgen, 1201 Court West, Mailstop 2262, Seattle, WA 98119-3105, USA.
§ Present address: Department of Inflammation, MedImmune Inc., Gaithersburg, MD 20878, USA.

0960-894X/$ - see front matter © 2006 Elsevier Ltd. All rights reserved.
doi:10.1016/j.bmcl.2006.05.056

One of the disturbing trends we observed from the outset of our p38 discovery effort was the large loss in potency when comparing the enzyme assay measuring p38 inhibition to a human whole blood (HWB) screen measuring TNF-α inhibition.[6] It is noteworthy to point out that many literature p38 inhibitors including SB-203580,[7] SB-242235,[8] RWJ-68354,[9,10] and VX-745[11] (see Fig. 1) exhibit this same phenomenon, and furthermore, that the difference in potency cannot be accounted for by correcting for protein binding. To the extent that HWB is a more realistic measure of potency this was a major concern for our program. Below we describe the structure–activity relationship for a series of triazolopyridines for which the HWB potency and ADME hurdles were overcome to identify compounds for clinical development.

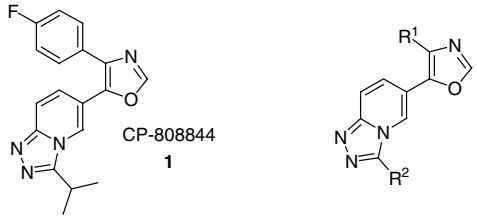

Figure 2. Triazolopyridine oxazoles.

Previously, we described the triazolopyridine-oxazole CP-808844 (Fig. 2) that was shown to bind to p38 with an unusual dual H-bond acceptor pattern,[13] While this configuration led to very good enzyme inhibition and may contribute to the excellent kinase selectivity for the series,[14] CP-808844 was not without problems. Foremost amongst these was the modest HWB potency (685 nM) which is masked by the excellent acute in vivo efficacy (rat TNF-α ED_{50} = 0.8 mg/kg),[15,16] consistent with the superior rat potency (rat whole blood IC_{50} = 92 nM). In addition, CP-808844 was metabolically unstable in human hepatic tissue, an attribute that could potentially contribute to poor pharmacokinetics in humans. As described herein, the narrowing of the gap between enzyme and HWB potency was solved in an empirical fashion and a clear understanding of HWB activity was never found. The human metabolic liability associated with CP-808844 was resolved in subsequent analogs guided by a detailed understanding of the biotransformation pathways.[17]

Three major areas were examined to improve the properties of the triazole series represented by CP-808844: the C4 aryl group (R^1), the side-chain (R^2), and the oxazole core ring (see Fig. 2). Shown in Table 1 are compounds with variations to the R^1 aryl group, a group thought to be one of the biggest contributors to the enzyme binding affinity for the compounds. Based on

Table 1. Triazolopyridine oxazole SAR: R^1 aryl group

Figure 2 Compound R^2 = *i*-Pr	R^1	p38α IC_{50} (nM)[c]	TNF-α cell IC_{50} (nM)[c]	TNFα HWB IC_{50} (nM)[c]
2[a]	Ph	9.6	71.4	973
3	3-Me-Ph	18.3	24.5	nd
4[a]	4-F-Ph	5.0	45.3	685
5[a]	3-F-Ph	37.8	135	nd
6[a]	4-F,5-Me-Ph	6.6	11.6	260
7[a]	2-F,5-Me-Ph	4.3	10.0	nd
8	4-Cl-Ph	17.7	70.0	nd
9	3-Cl-Ph	13.5	52.3	550
10	2-Cl-Ph	3.0	57.4	937
11[a]	2,4-diF-Ph	4.6	10.0	265
12[b]	2,5-diF-Ph	5.8	25.0	259
13[b]	2,6-diF-Ph	14.6	71.1	nd
14	3,4-diF-Ph	22.3	49.0	nd
15[b]	3-Cl,4-F-Ph	12.4	47.2	631
16[a]	2-F,4-Cl-Ph	2.2	20.0	600
17	2-F,5-Cl-Ph	5.1	10.0	190
18[b]	2-Cl,4-F-Ph	2.5	24.5	380
19	3-F,4-Cl-Ph	43.2	266	nd
20[b]	3,4,5-triF-Ph	4.1	480	nd
21[b]	2,4,5-triF-Ph	3.2	19.7	263
22[b]	2,4,6-triF-Ph	7.2	60.0	650
23[b]	2,3,5-triF-Ph	83.3	490	nd
24	2,3,4-triF-Ph	11.1	57.4	nd
25	3,4-diCl-Ph	26.4	148	nd
26[b]	2,4-diCl-Ph	8.3	30.0	nd
27[b]	2,3-diCl-Ph	14.5	57.4	nd
28[b]	2-F,4-Cl,5-F-Ph	24.5	60.0	nd
29[b]	2-Cl,4-F,5-F-Ph	5.6	54.8	nd
30[b]	3-Br,4-F-Ph	8.0	122	nd

nd, not determined.

[a] Human hepatocyte extraction ratio (Er_H) > 0.5.

[b] Human microsome and hepatocyte Er_H < 0.3.

[c] IC_{50}s are reported as the geometric mean of three or more experiments. Standard deviations for the assays are generally ±30% of the mean or less.

structural data.[18] substitutions on this aryl ring were confined to non-polar groups. The synthesis of the compounds (Tables 1 and 2) followed the chemistry already described for CP-808844.[13] What emerged from this work is that close-in combinations of fluoro- or chlorophenyl substituents were enough to give important improvements in both trouble areas for the lead structure. Preferred fluoro substitution patterns are 2,4 and 2,5 and 2,4,5. Combinations with one chloro and one fluoro were also well tolerated, especially with the same 2,4 and 2,5 substitution patterns. Poor monocyte cell potency[19] was generally predictive of poor HWB activity (see **2**, **46**, **54**, and **65**), but the reverse was not always true (see **55**, **56**, Table 2). Interestingly, changes in substitution patterns also increased the human microsomal stability often in spite of large increases in lipophilicity.

Table 2. Triazolopyridine oxazole SAR: R^2 side-chain

Figure 2 Compound	R^2	p38α IC_{50} (nM)[c]	TNFα cell IC_{50} (nM)[c]	TNFα blood IC_{50} (nM)[c]
R^1 = Ph				
31[a]	Et	54.5	672	nd
32[a]	c-Propyl	47.2	150	nd
33	c-Bu	16.6	69.3	nd
34[a]	EtNH	5.4	40.0	1707
35[a]	EtMeN	9.2	80.0	nd
36	F_2CH	544	nd	nd
37[a]	CF_3CH2	83.2	915	nd
38	Isoxazol-5-yl	285	> 2000	nd
R^1 = 4-F-Ph				
39[b]	H	19.5	>5000	nd
41	Et	21.6	630	nd
42[a]	Me_2N	15.3	165	nd
43	EtNH	7.6	52	865
44	EtO	55.5	360	nd
45[a]	c-Bu	17.7	49	nd
46[a]	c-Propyl	10.9	186	4650
47	*i*-Bu	8.8	70	nd
48	*i*-PrNH	5.5	31.6	nd
49	*n*-Pr-NH	198	nd	nd
50	MeEtN	4.7	34.6	1553
51	*i*-PrO	17.9	470	nd
52[a]	1-Me-c-butyl	14.0	40.0	nd
53[a]	pyrrolidine	15.4	52.0	935
54[a]	Ph	12.3	90.0	5350
55	2-MeOPh	0.4	10	873
56[a]	2-EtO-Ph	0.4	10	697
57[b]	*t*-Bu	3.5	38.7	470
58[b]	Morpholine	11.8	1440	nd
59	$PhCH_2$	19.9	>1000	nd
R^1 = 2,4-diF-Ph				
60	c-Propyl	3.5	45.8	910
61[a]	1-Me-c-propyl	0.7	30	245
62[a]	c-Butyl	3.75	40	nd
63	1-Me-c-butyl	1.1	10	77
64[b]	*t*-Bu	1.1	12.6	76
R^1 = 2,5-diF-Ph				
65	2-propanol-2-yl	25	200	1395
66[b]	c-Propyl	24.0	31.6	1400
67[b]	1-Me-c-propyl	3.0	45.8	385
68	c-Butyl	9.7	60	nd
69	1-Me-c-butyl	1.5	10	nd
70[b]	*t*-Bu	8.8	14.1	220
R^1 = 2,4,5,-triF-Ph				
71[b]	c-Propyl	7.8	40	565
72[b]	1-Me-c-propyl	2.3	28.3	263
73	c-Butyl	9.1	50	353
74	1-Me-c-butyl	2.5	10	90
75[b]	*t*-Bu	1.8	8.3	63

nd, not determined.

[a] Human hepatocyte extraction ratio (Er_H) > 0.5.

[b] Human microsome and hepatocyte Er_H < 0.3.

[c] IC_{50}s are reported as the geometric mean of three or more experiments. Standard deviations for the assays are generally ±30% of the mean or less.

For example, the majority of di-halo compounds in Table 1 were more stable than the mono-fluoro compounds **4** and **5**. Considering that oxidative metabolism on the isopropyl and the oxazole group were the primary routes of biotransformation,[17] a potential explanation for the improved metabolic stability is that the C4 aryl substitution decreases the affinity of the compounds for the cytochrome P450 responsible for metabolism. Alternatively, an inductive effect by the C4 aryl group could potentially deactivate the oxazole ring toward oxidative metabolism.

Encouraged by these initial findings we incorporated variations to the side-chain R^2 (Table 2). In terms of HWB potency a trend emerged favoring quaternary-branched alkyl or cycloalkyls (cf. R^2 = *i*-Pr to *t*-Bu, cyclopropyl to 1-methylcyclopropyl and cyclobutyl to 1-methylcyclobutyl). In some cases less than a 30-fold loss in potency is observed from the enzyme to the HWB assay. Since P450-mediated oxidation of the R^2 substituent was also a major route of metabolism in the series, it is perhaps not surprising that changes to this area of the molecule had influence on the metabolism. One such example can be seen with **57** and **58** relative to **1**. It is tempting to think that groups such as R^2 equal to *t*-Bu lead to a general improvement in metabolic stability but this interpretation is complicated by the fact that the R^1 aryl group also contributes to the overall stability of the compounds.

The final region targeted for evaluation was the central oxazole ring and a limited comparison of five-membered ring heterocycles is shown in Table 3. The synthesis of these analogs is shown in Schemes 1 and 2. As outlined in Scheme 1 the aldehyde **76** was reacted with the *N*,*P*-acetal **77**[20] to give the intermediate ketone **78** in poor yield. The ketone was then used to prepare either the pyrazole **79** or the isoxazole **80** by formylation with *N*,*N*-dimethylformamide dimethyl acetal (DMF-DMA) and subsequent reaction with either hydrazine or hydroxylamine as appropriate.

The imidazole **81** was prepared in one step as shown in Scheme 2.[21] Alternative conditions employing aqueous ammonium hydroxide described for pyridyl-imidazoles[22] led primarily to the Dimroth rearranged triazolo-pyridine-imidazole product **82**.[13]

Table 3. Core ring SAR and Caco-2 permeability

Schemes 1 and 2 Compound and **12**	p38α IC_{50} (nM)[a]	TNF-α cell IC_{50} (nM)[a]	TNF-α blood IC_{50} (nM)[a]	Caco-2 AB/BA[b]
79	2.8	14.1	180	6/18
80	33.2	63	nd	41/29
81	6.2	24.5	297	1/32
12		Table 1		43/29

nd, not determined.

[a] IC_{50}s are reported as the geometric mean of three or more experiments. Standard deviations for the assays are generally ±30% of the mean or less.

[b] AB, flux from apical to basolateral ($\times 10^{-6}$ cm/s). BA, rate in reverse direction.

The imidazole and pyrazole analogs **81** and **79** have in vitro potencies comparable to their oxazole counterpart (Table 3). Unlike the oxazole **12**, however, they both show unfavorable absorption in the Caco-2 permeability screen (predicted oral absorption <10% based on the flux from the apical to the basolateral direction). Furthermore, the observation that the rate of translocation from the basolateral to the apical side of the Caco-2 cells significantly exceeds the flux from apical to basolateral suggests that the two compounds may be substrates for efflux transport proteins such as p-glycoprotein. In contrast, the isoxazole **80** lacking the H-bond donor present in **79** and **81** did exhibit good Caco-2 permeability but was a considerably less potent p38 inhibitor. Although specific in vivo studies were not performed to reaffirm the Caco-2 findings on poor oral absorption, the in vivo rat TNF-α activity for the pyrazole and imidazole analogs after oral absorption was generally inferior to their oxazole comparators.

Based on overall in vitro properties a number of compounds were evaluated for their overall pharmacokinetic profiles. As shown in Table 4 the selected compounds have low to moderate plasma clearance (CL_p) and volume of distribution at steady state (V_{dss}) in the rat and monkey that translated into low to moderate terminal half-lives in these species. In general, the compounds also exhibited moderate bioavailability.

In the case of **9** and **15** the lower bioavailabilities may be attributable to their very poor thermodynamic solubility (Table 5). Based on molecular weight (MW = 322) and measured physicochemical properties of CP-808844 ($\log D = 2.18$; $pK_a = 2.86$) there was no particular reason to suspect solubility as an issue for the series. As shown in Table 5 melting points were only partially predictive of the solubility. Interestingly, not only did the presence of *m*-chloro group on the aromatic have a significant influence on solubility it had a measurable effect on the inhibition of the human *ether-a-go-go*-related gene (hERG) channel expressed in human embryonic kidney (HEK-293) cells (cf. **1**, **9**, **15**, and **18**).[23] This could be explained by some specific hydrophobic contact, but it is also possible that it is a substituent tuning of a π–π interaction[24] given that such interactions are one of the most important with hERG.[25] While the very poor solubility of **15** was not enough to halt its progression, taken together with the observed inhibition of hERG forced a consideration of other compounds. In this regard, the acute in vivo activity was not particularly discriminating and needed to be placed in the context of drug concentrations and their relationship to efficacy in human systems. To this end the HWB potency was used as a key selection criterion. On this basis a number of compounds looked more promising than **15**. The combined attributes of **12** and **75** including their performance in other acute and chronic models of inflammation led to their selection for clinical development.

In summary, the evolution of the lead structure CP-808844 to compounds suitable for clinical evaluation was described. One of the significant observations is

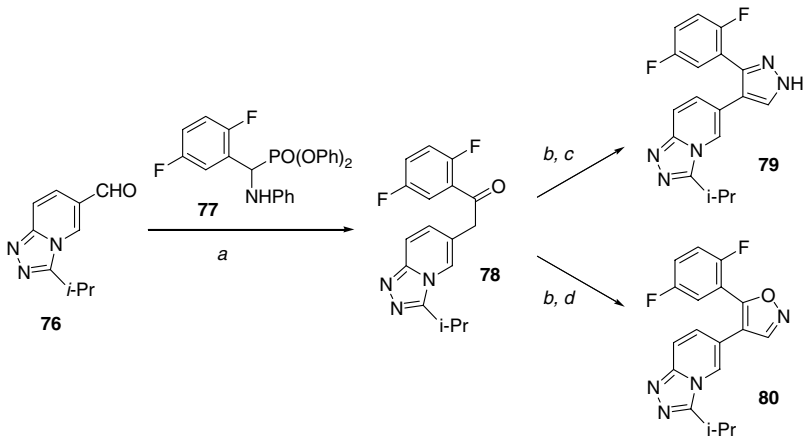

Scheme 1. Synthesis of pyrazole and isoxazole triazolopyridines. Reagents and conditons: (a) KO*t*-Bu, THF/*i*-PrOH, 23 °C, 45 min, then aqueous HCl (39%); (b) DMF–DMA, 90 °C, 1 h, (100%); (c) hydrazine hydrate, EtOH/H_2O, 70 °C, 30 min, 56%; (d) NH_2OH HCl, KOAc, EtOH, reflux, 2 h, 58%.

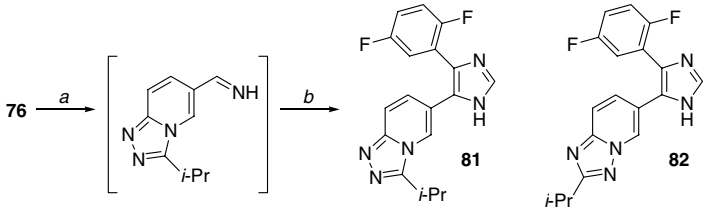

Scheme 2. Synthesis of triazolopyridines-imidazoles. Reagents and conditions: (a) LiHMDS, THF, −40 °C, 1 h, then; (b) α-(*p*-toluenesulfonyl)-2,5-difluorobenzyl-isonitrile, 22 °C, 18 h, 16%.

Table 4. Rat and monkey pharmacokinetics after intravenous and oral administration

Figure 2 Compound	CL_p (mL/min/kg)	V_{dss} (L/kg)	$t_{1/2}$ (h)	*F* (%)
Rat				
1	12	0.8	0.7	85
9	17	1	1.6	37
12	14	0.8	1.3	58
15	17	1.3	0.9	9.4
75	3	0.6	2.6	54
Monkey				
1	16	1.8	1.3	75
9	15	1	1.1	19
12	6.0	1.3	5.4	40
15	5.7	1.4	4.7	31
75	3.4	1.2	5.2	66

the high similarity of CP-808844 to the more optimized structures. Also noteworthy is the repeated occurrence of large pharmacological, metabolic, or physical changes attributable to small structural differences. Ultimately, a number of promising compounds with similar overall profiles were identified. From these compounds, **12** and **75** were selected for development with an emphasis on their potency in HWB.

Table 5. Solubility, melting point, hERG, and in vivo SAR

Figure 2 Compound	Equilibrium solubility[a] (μg/mL)/melting point (°C)	Inhibition of hERG current at 3 μM (%)	Rat LPS-TNFα ED_{50} (mg/kg)
1	29.6/212	0	0.8
9	5.2/228–231	14	2.4–3
12	8.1/174	0 (at 1 μM)	0.3
15	2.8/227–228[b]	49	0.5
18	81/191–192	0	94% inhib[c]
75	41/177	5.9	0.1

[a] PBS, phosphate buffered saline pH 6.5.
[b] As HCl salt.
[c] at 3 mg/kg.

References and notes

1. Lee, J. C.; Laydon, J. T.; McDonnell, P. C.; Gallagher, T. F.; Kumar, S.; Green, D.; McNulty, D.; Blumenthal, M. J.; Heys, J. R.; Landvatter, S. W., et al. *Nature* **1994**, *372*, 739.
2. Dominguez, C.; Tamayo, N.; Zhang, D. *Expert Opin. Ther. Patents* **2005**, *15*, 801.
3. Fijen, J. W.; Zijlstra, J. G.; De Boer, P.; Spanjersberg, R.; Cohen Tervaert, J. W.; Van Der Werf, T. S.; Ligtenberg, J. J.; Tulleken, J. E. *Clin. Exp. Immunol.* **2001**, *124*, 16.
4. Kim, A. L.; Labasi, J. M.; Zhu, Y.; Tang, X.; McClure, K.; Gabel, C. A.; Athar, M.; Bickers, D. R. *J. Invest. Dermatol.* **2005**, *124*, 1318.

5. Kotlyarov, A.; Neininger, A.; Schubert, C.; Eckert, R.; Birchmeier, C.; Volk, H. D.; Gaestel, M. *Nat. Cell Biol.* **1999**, *1*, 94.
6. All HWB IC_{50}s reported herein were measured as follows: whole blood was collected into heparinized tubes (30 U/mL). Compounds were prepared in DMSO at 5000, 50, and 5 mM. DMSO stocks were diluted 50× in RPMI containing 200 mM HEPES. Into a 96-well U-bottom plate, 12.5 μL of diluted compound, 12.5 μL LPS (2.0 mg/mL-serotype 055:B5, Sigma–Aldrich), and 225 μL of heparinized blood were added. The plate was incubated at 37 °C/5.0% CO_2 for 4 h. Plasma was assessed for TNF-α by ELISA (R&D Systems).
7. Boehm, J. C.; Smietana, J. M.; Sorenson, M. E.; Garigipati, R. S.; Gallagher, T. F.; Sheldrake, P. L.; Bradbeer, J.; Badger, A. M.; Laydon, J. T.; Lee, J. C.; Hillegass, L. M.; Griswold, D. E.; Breton, J. J.; Chabot-Fletcher, M. C.; Adams, J. L. *J. Med. Chem.* **1996**, *39*, 3929.
8. Badger, A. M.; Griswold, D. E.; Kapadia, R.; Blake, S.; Swift, B. A.; Hoffman, S. J.; Stroup, G. B.; Webb, E.; Rieman, D. J.; Gowen, M.; Boehm, J. C.; Adams, J. L.; Lee, J. C. *Arthritis Rheum.* **2000**, *43*, 175.
9. Henry, J. R.; Rupert, K. C.; Dodd, J. H.; Turchi, I. J.; Wadsworth, S. A.; Cavender, D. E.; Schafer, P. H.; Siekierka, J. J. *Bioorg. Med. Chem. Lett.* **1998**, *8*, 3335.
10. Henry, J. R.; Rupert, K. C.; Dodd, J. H.; Turchi, I. J.; Wadsworth, S. A.; Cavender, D. E.; Fahmy, B.; Olini, G. C.; Davis, J. E.; Pellegrino-Gensey, J. L.; Schafer, P. H.; Siekierka, J. J. *J. Med. Chem.* **1998**, *41*, 4196.
11. Haddad, J. J. *Curr. Opin. Investig. Drugs* **2001**, *2*, 1070.
12. All enzyme IC_{50}s were determined as described in: Dombroski, M. A.; Letavic, M. A.; McClure, K. F.; Barberia, J. T.; Carty, T. J.; Cortina, S. R.; Csiki, C.; Dipesa, A. J.; Elliott, N. C.; Gabel, C. A.; Jordan, C. K.; Labasi, J. M.; Martin, W. H.; Peese, K. M.; Stock, I. A.; Svensson, L.; Sweeney, F. J.; Yu, C. H. *Bioorg. Med. Chem. Lett.* **2004**, *14*, 919.
13. McClure, K. F.; Abramov, Y. A.; Laird, E. R.; Barberia, J. T.; Cai, W.; Carty, T. J.; Cortina, S. R.; Danley, D. E.; Dipesa, A. J.; Donahue, K. M.; Dombroski, M. A.; Elliott, N. C.; Gabel, C. A.; Han, S.; Hynes, T. R.; LeMotte, P. K.; Mansour, M. N.; Marr, E. S.; Letavic, M. A.; Pandit, J.; Ripin, D. B.; Sweeney, F. J.; Tan, D.; Tao, Y. *J. Med. Chem.* **2005**, *48*, 5728.
14. The representative compounds **2**, **18**, **21**, **43**, **64**, **75**, **79** have IC_{50}s > 10 μM against the following kinases: p38γ, p38δ, MKK1, MAPK2/ERK2, JNK, MAPKAP-K1a, MAPKAP-K2, MSK1, PRAK, PKA, PKCα, PDK1, PKBα, SGK, P70S6K, GSK3β, ROCK-II, AMPK, CHK1, CK2, Lck, CSK, CDK2, PI3-K, DYRK1a, PHOS. Kinase.
15. All procedures were reviewed and approved by the Institutional Animal Care & Use Committee.
16. Unless otherwise noted all in vivo pharmacology reported herein was conducted as follows: rats were weighed and dosed with vehicle (0.5% methyl cellulose, Sigma) or drug. One hour later, animals were injected i.p. with LPS (50 mg/rat, Sigma L-4130). Ninety min later, animals were euthanized by asphyxiation with CO_2 and bled by cardiac puncture. Blood was collected in Vaccutainer tubes and spun for 20 min at 3000 rpm. Serum was assayed for TNF-α levels using an ELISA (R& D Systems).
17. Kalgutkar, A. S.; Hatch, H. L.; Kosea, F.; McClure, K. F.; Dombroski, M. A.; Choo, E. F.; Henne, K. R.; Taylor, T. J.; Kuperman, A. V. *Boopharm. Drug Dispos.* Manusscript in press.
18. PDB accession code 1ZZL.
19. Mononuclear cells were isolated from the heparainized whole blood of healthy volunteers using Sigma–Aldrich Accuspin tubes. Fifty microliters of 2×10^6 cells in RPMI medium containing 5% FBS was added to each well of 96-well plate. Five millimolar DMSO stocks of test agents were diluted in the 5% FBS/RPMI medium containing 200 ng/mL LPS with a final DMSO concentration of 0.4%. Fifty microliters of the diluted test compound was added to each well. Plates were incubated for 4 h at 37 °C, 5% CO_2. After 4 h, cell supernatants were harvested by centrifugation and TNF-α concentration determined by ELISA (R&D).
20. Davies, I. W.; Marcoux, J. F.; Corley, E. G.; Journet, M.; Cai, D. W.; Palucki, M.; Wu, J.; Larsen, R. D.; Rossen, K.; Pye, P. J.; DiMichele, L.; Dormer, P.; Reider, P. J. *J. Org. Chem.* **2000**, *65*, 8415.
21. Shih, N.-Y. *Tetrahedron Lett.* **1993**, *34*, 595.
22. Sisko, J.; Kassick, A. J.; Mellinger, M.; Filan, J. J.; Allen, A.; Olsen, M. A. *J. Org. Chem.* **2000**, *65*, 1516.
23. Volberg, W. A.; Koci, B. J.; Su, W.; Lin, J.; Zhou, J. *J. Pharmacol. Exp. Ther.* **2002**, *302*, 320.
24. Sinnokrot, M. O.; Sherrill, C. D. *J. Am. Chem. Soc.* **2004**, *126*, 7690.
25. Sanchez-Chapula, J. A.; Navarro-Polanco, R. A.; Culberson, C.; Chen, J.; Sanguinetti, M. C. *J. Biol. Chem.* **2002**, *277*, 23587.